An ultra-low-power CMOS temperature sensor for RFID applications

Xu Conghui(徐琮辉), Gao Peijun(高佩君), Che Wenyi(车文毅), Tan Xi(谈熙), Yan Na(闫娜)†, and Min Hao(闵昊)

(State Key Laboratory of ASIC & System, Fudan University, Shanghai 201203, China)

Abstract: An ultra-low-power CMOS temperature sensor with analog-to-digital readout circuitry for RFID applications was implemented in a 0.18-μm CMOS process. To achieve ultra-low power consumption, an error model is proposed and the corresponding novel temperature sensor front-end with a new double-measure method is presented. Analog-to-digital conversion is accomplished by a sigma-delta converter. The complete system consumes only 26 μA @ 1.8 V for continuous operation and achieves an accuracy of ±0.65 °C from –20 to 120 °C after calibration at one temperature.

Key words: CMOS temperature sensor; error analysis; digital output; low power; RFID
DOI: 10.1088/1674-4926/30/4/045003 **EEACC:** 1205; 1065H

1. Introduction

RFID technology has attracted profound attention. Not content with object identification only, people are seeking for more functions provided by RFID systems. One of the most attractive applications is to realize real-time temperature sensing by integrating a temperature sensor into the RFID tag. However, there exist some challenging features for the sensor. First, the temperature sensor must be on-chip and easy to calibrate to minimize the cost. Second, the power consumption of the sensor is stringently limited. Third, the temperature sensor should achieve high accuracy in the whole temperature sensing range.

Several papers have reported temperature sensor designs. However, these can either not be realized in low-cost CMOS technology[1] or they consume too much power for continuous operation[2–5]. In this paper, a novel design of a CMOS temperature sensor, which offers low power, low cost and high accuracy, is proposed. An error model for this sensor is developed. Also, the architectural improvements of the temperature sensor, which includes a sensor front-end and a sigma-delta ADC, is given.

2. Error model

The most important candidate for a CMOS temperature sensor is the bipolar transistor, which can be realized as a parasitic device in standard CMOS technology[2–5]. Almost all CMOS temperature sensors follow the principle of the general architecture of the bandgap reference as illustrated in Fig. 1.

The difference of the two base-emitter voltages is direct proportional to the absolute temperature (PTAT), as given by

$$V_{\rm PTAT} = V_{\rm BE}(I_1) - V_{\rm BE}(I_2) = \frac{kT}{q}\ln\frac{I_1}{I_2}. \tag{1}$$

Therefore, the temperature can be measured by comparing $V_{\rm PTAT}$ with the reference voltage, which is theoretically temperature independent. Nevertheless, several errors are inherent in such a circuit, and thus the accuracy greatly depends on the process parameters. A typical test result for the errors of CMOS temperature sensor is presented in Ref. [5] and listed in Table 1.

As shown, the errors of this bandgap reference circuit are due to the offset of the opamp $\sigma(V_{\rm os})$, the spread in the absolute value of the base–emitter voltage $\sigma(V_{\rm be})$, the spread in the absolute value of the resistors $\sigma(R_{\rm sh})$, the mismatch of the bipolar transistor $\sigma(V_{\rm os}, Q)$, and the mismatch of the resistors $\sigma(\Delta R)$, respectively.

A temperature sensor error model was built according to the test results described in Table 1 with the error sources being expressed as

$$\sigma(V_{\rm os}):\ V_{\rm offset} = \sigma_{\rm offset}, \tag{2}$$

Table 1. Errors of the bandgap reference circuit in Ref.[5].

Kind of error	Typical value	Error contribution for typical value
$\sigma(V_{\rm os})$	0.4 mV	2 °C
$\sigma(V_{\rm os}, Q)$	0.1 mV	0.5 °C
$\sigma\triangle R$	0.1%	0.15 °C
$\sigma(R_{\rm sh})$	4%	0.25 °C
$\sigma(V_{\rm be})$	2 mV	0.5 °C

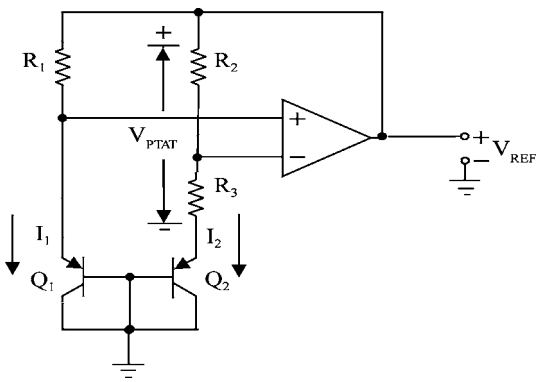

Fig. 1. General architecture of a bandgap reference.

† Corresponding author. Email: yanna@fudan.edu.cn
Received 24 September 2008, revised manuscript received 3 December 2008

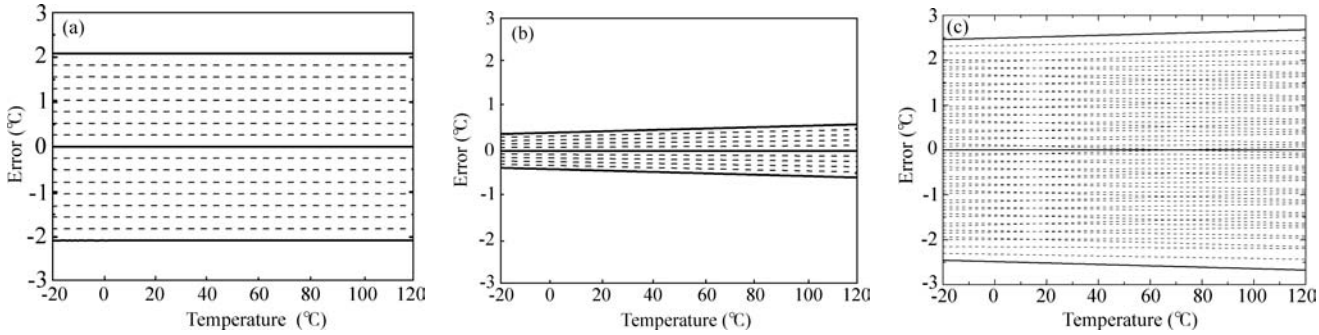

Fig. 2. Errors in a bandgap reference circuit caused by (a) opamp offset, (b) mismatch of the bipolar transistors, and (c) both.

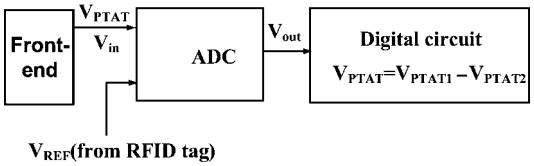

Fig. 3. Block diagram of the temperature sensor.

$$\sigma(V_{be}):\ V_{BE} = V_T \ln \frac{I}{I_S(1+\sigma_{BE})}, \tag{3}$$

where $V_T = kT/q$. The difference between $\sigma_{BE\text{-}Q1}$, representing the $\sigma(V_{be})$ of the bipolar transistor Q1, and $\sigma_{BE\text{-}Q2}$, representing the $\sigma(V_{be})$ of the bipolar transistor Q2, denotes the mismatch of the bipolar transistors $\sigma(V_{os},Q)$.

$$\sigma(R_{sh}):\ R = R(1+\sigma_R). \tag{4}$$

Similarly, the difference between σ_{R1} and σ_{R2}, which is the $\sigma(R_{sh})$ of resistors R_1 and R_2, respectively, denotes the mismatch of the resistors $\sigma(\Delta R)$.

The simulation of the errors $\sigma(V_{os})$ and $\sigma(V_{os}, Q)$ are illustrated in Figs. 2(a) and 2(b), respectively, when setting the ratio of I_1 and I_2 to be a typical value of eight. The results matched well with the data given in Table 1. Figure 2(c) shows $\sigma(V_{os})$ and $\sigma(V_{os}, Q)$ as functions of temperature. As shown, the error varies ±2.5 °C in the range of −20 to 120 °C.

Based on Eqs. (2)–(4), the reference voltage and the temperature dependent voltage illustrated in Fig. 1 are given by

$$V_{PTAT} = \left\{ V_T \left[\ln \frac{I_1}{I_2} - \ln \frac{1+\sigma_{BE\text{-}Q1}}{1+\sigma_{BE\text{-}Q2}} \right] + \sigma_{offset} \right\} \left[1 + \frac{R_3(1+\sigma_{R3})}{R_2(1+\sigma_{R2})} \right] \tag{5}$$

$$V_{REF} = V_{BE\text{-}Q2} + AV_{PTAT} = V_{BE-Q2} + A \left\{ V_T \left[\ln \frac{I_1}{I_2} - \ln \frac{1+\sigma_{BE\text{-}Q1}}{1+\sigma_{BE\text{-}Q2}} \right] + \sigma_{offset} \right\} \left[1 + \frac{R_3(1+\sigma_{R3})}{R_2(1+\sigma_{R2})} \right], \tag{6}$$

where A is a coefficient. It is shown that the reference voltage V_{REF} is affected by $\sigma(V_{os})$, $\sigma(V_{os}, Q)$, $\sigma(\Delta R)$, and $\sigma(V_{be})$, while the temperature dependent voltage V_{PTAT} is only affected by $\sigma(V_{os})$, $\sigma(V_{os}, Q)$, and $\sigma(\Delta R)$.

3. Architecture improvement

As illustrated in Fig. 3, the temperature sensor front-end generates the temperature dependent voltage V_{PTAT}, which is the input signal of a second-order sigma-delta ADC. The reference voltage for ΣΔADC is generated from the RFID tag. After ΣΔADC digitalizes V_{PTAT}, the digital circuit calculates the difference of V_{PTAT} for two working modes of the front-end circuit.

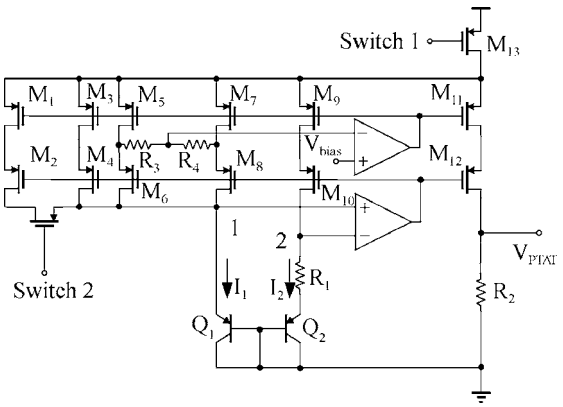

Fig. 4. The proposed novel temperature sensor front-end.

3.1. CMOS temperature sensor front-end

To achieve high accuracy and low power, we propose a novel temperature sensor front-end, as illustrated in Fig. 4. The output voltage is also temperature dependent and given by

$$V_{PTAT} = (V_{BE\text{-}Q1} - V_{BE\text{-}Q2}) \frac{R_2(1+\sigma_{R2})}{R_1(1+\sigma_{R1})} = \left\{ V_T \left[\ln \frac{I_1}{I_2} - \ln \frac{1+\sigma_{BE\text{-}Q1}}{1+\sigma_{BE\text{-}Q2}} \right] + \sigma_{off} \right\} \frac{R_2(1+\sigma_{R2})}{R_1(1+\sigma_{R1})}. \tag{7}$$

The Switch 2 controls the value of I_1. I_1 is four times larger than I_2 when the Switch 2 is closed. While the Switch 2 is open, I_1 is three times larger than I_2. So the difference of V_{PTAT} between two working modes is

$$\Delta V_{PTAT} = V_{PTAT1} - V_{PTAT2} = \frac{kT}{q} \ln\left(\frac{4}{3}\right) \frac{R_2(1+\sigma_{R2})}{R_1(1+\sigma_{R1})}. \tag{8}$$

The result implies a good performance of this new double-measure method. The only error of the voltage difference, which is proportional to the absolute temperature, comes from the mismatch of the resistances, namely $\sigma(\Delta R)$, which is well controlled in CMOS technology.

However, V_{PTAT} is digitalized by ΣΔADC by comparing it with V_{REF}. So the accuracy of ΔV_{PTAT} also depends on the precision of the reference voltage, which is provided by a bandgap circuit in the RFID tag. As seen from Eq. (4), it is

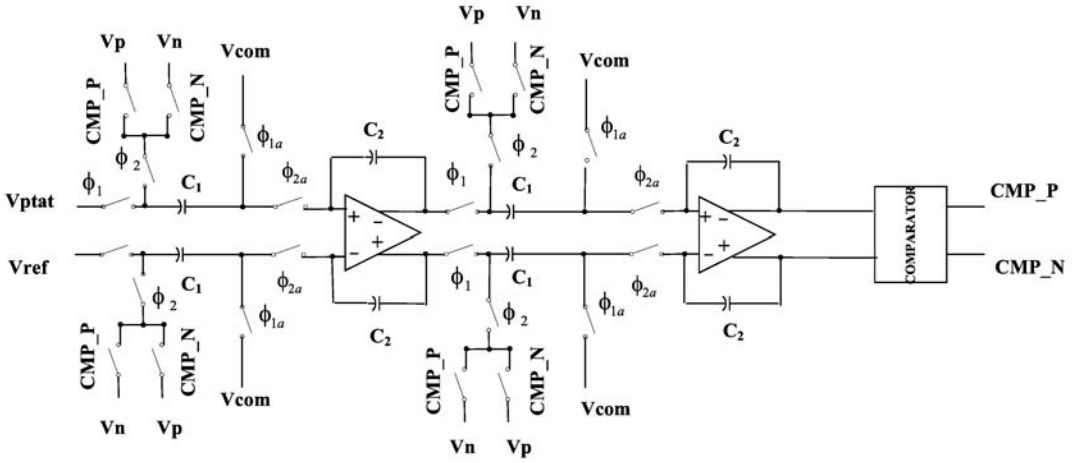

Fig. 5. Second-order sigma-delta modulator.

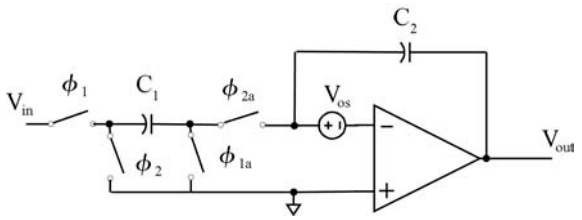

Fig. 6. Sample-and-hold circuit in the second-order sigma-delta modulator.

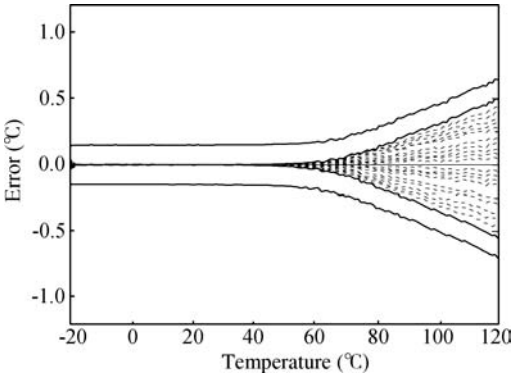

Fig. 7. Errors in the proposed temperature sensor.

difficult to keep $V_{\rm REF}$ constant over a large temperature range and usually requires complex calibrations such as second-order curvature correction[4]. Fortunately, the fact that temperature sensing and recording is discrete in time alleviates this demand. By comparing $V_{\rm PTAT}$ for two working modes with the same reference voltage, the difference voltage $\Delta V_{\rm PTAT}$ can be precisely measured when $V_{\rm REF}$ is equal in just two cases rather than requiring $V_{\rm REF}$ to be exactly the same over the whole measured temperature range. Thus, a calibration for $V_{\rm REF}$ is no longer necessary. As is shown in Eq. (6), the proposed temperature sensor front-end has the advantage of better immunity to the main errors of $\sigma(V_{\rm os})$, $\sigma(V_{\rm os}, Q)$, $\sigma(V_{\rm be})$, and $\sigma(R_{\rm sh})$. A sigma-delta ADC following the circuit is designed to digitize the $V_{\rm PTAT}$ for two working modes.

3.2. AD converter

The sigma-delta ADC has been proven to be very suitable in low-frequency, high-performance cases. In our application, the signal almost acts as a DC signal. A second-order sigma-delta ADC is chosen for its low complexity and moderate accuracy of 10 bits.

Nevertheless, the offset in the sigma-delta modulator would influence the DC signal. As shown in Fig. 6, the output voltage would include the offset voltage of the opamp when sampling the input signal in a sample-and-hold (S-H) circuit. The output voltage is given by

$$V_{\rm out} = \frac{C_1}{C_2}V_{\rm in} + 1 + \frac{C_1}{C_2}V_{\rm os}. \quad (9)$$

As $V_{\rm os}$ is constant regardless of the switch 2 in Fig. 4 being closed or open, we can write

$$\Delta V_{\rm out} = V_{\rm out1} - V_{\rm out2} = \frac{C_1}{C_2}(V_{\rm in1} - V_{\rm in2}) = \frac{C_1}{C_2}\Delta V_{\rm PTAT}. \quad (10)$$

The offset voltage of the opamp is cancelled automatically and does not induce additional errors when converting the analog DC signal to the digital domain.

3.3. Architecture error simulation

The proposed architecture overcomes the error sources of $\sigma(V_{\rm os})$, $\sigma(V_{\rm os}$, Q), $\sigma(V_{\rm be})$, and $\sigma(R_{\rm sh})$ described in the error model. As illustrated in Fig. 7, the temperature error in the most interested range of –20 to 50 °C is negligible. The remaining error $\sigma(\Delta R)$ caused a ±0.65 °C variation in the range of –20 to 120 °C due to the mismatch of R_1 and R_2.

4. Measurement results

The whole CMOS temperature sensor is implemented in SMIC 0.18-μm RF process. The micrograph of this proposed sensor is shown in Fig. 8. The complete circuit occupies 0.9 mm^2 (excluding bond pads).

The measured results for the proposed temperature sensor, which are illustrated in Fig. 9, matches well with the simulation results. After calibration at one temperature, the variation of the error is less than ±0.65 °C from –20 to 120 °C. To meet the stringent limit of power consumption of the RFID

Table 2. Comparison with previous work.

Reference	Power consumption	Inaccuracy	Range	Calibration
Bakker[2]	N.A. for continuous operation 25 μA at 50 conversions/s 3 μA at 2 conversions/s	±1.0 °C	–40 to 120 °C	2 points
Tuthill[3]	1 mA for continuous operation 0.3 μA at 10 conversions/s	±1.0 °C	–50 to 125 °C	1 point
Pertijs[4]	N.A. for continuous operation 130 μA at 10 conversions/s	±0.5 °C	–50 to 125 °C	1 point
This work	26 μA for continuous operation 0.2 μA at 1 conversions/s	±0.65 °C	–20 to 120 °C	1 point

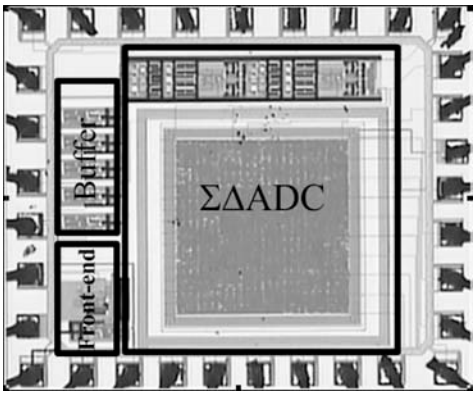

Fig. 8. Micrograph of the proposed temperature sensor.

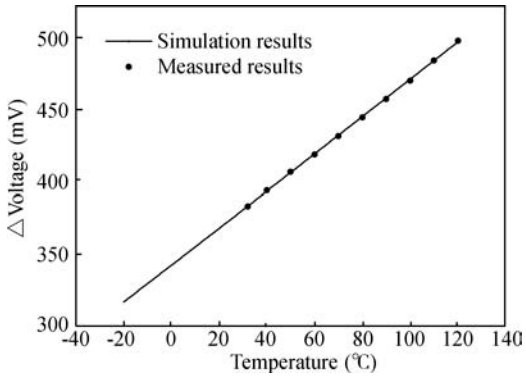

Fig. 9. Measured output voltage for the proposed temperature sensor.

tag, the sensor with digital output consumes only 26 μA @ 1.8 V for continuous operation, of which 6 μA is consumed by the sensor front-end and 20 μA by the sigma-delta converter.

Table 2 compares the power consumption, the inaccuracy and calibration condition with previous works. Many temperature sensors provide an additional low-power working mode in which the sensor is normally shut down and only powers up when necessary. As the time for one temperature measurement is usually only several ten microseconds, the average power consumption is far less than the peak one[3]. For continuous operation the power consumption should be limited to 50 μA for RFID applications. Our work also provides an additional low-power working mode controlled by Switch 1 in Fig. 4. The presented temperature sensor performs as well as sensors presented in previous works over a wide temperature range, but achieves much lower power consumption for continuous operation.

5. Conclusion

The temperature sensor with digital output for RFID applications offers limited power consumption, low cost and high accuracy. A novel design of a CMOS temperature sensor is presented. Compared with traditional power-hungry error-cancellation technologies such as Dynamic Element Matching (DEM) of bias current[2−5], the proposed sensor front-end with a second-order sigma-delta ADC overcomes the circuit errors by means of a new double-measure method and consumes only 26 μA @ 1.8 V for continuous operation. After calibration at one temperature, the sensor achieves an accuracy of ±0.65 °C in the measured temperature range from –20 to 120 °C.

Acknowledgments

The authors would like to thank Lee Yang of SMIC (Shanghai) for chip fabrication support.

References

[1] Soto M A, Sahu P K, Rueck C, et al. Distributed temperature sensor system based on Raman scattering using correlation-codes. Electron Lett, 2007, 43(16): 862

[2] Bakker A, Huijsing J H. Micropower CMOS temperature sensor with digital output. IEEE J Solid-State Circuits, 1996, 31(7): 933

[3] Tuthill M. A switched-current, switched-capacitor temperature sensor in 0.6-μm CMOS. IEEE J Solid-State Circuits, 1998, 33(7): 1117

[4] Pertijs M A P, Niederkorn A, Ma X, et al. A CMOS smart temperature sensor with a 3σ inaccuracy of ±0.5 °C from −50 °C to +120 °C. IEEE J Solid-State Circuits, 2005, 40(2): 454

[5] Bakker A, Huijsing J H. A low-cost high-accuracy CMOS smart temperature sensor. Proceedings of the 25th European ESSCIRC, 1999: 302